MIUA2015

Medical Image Understanding and Analysis 2015

Editors:
Dr Tryphon Lambrou
and Dr Xujiong Ye

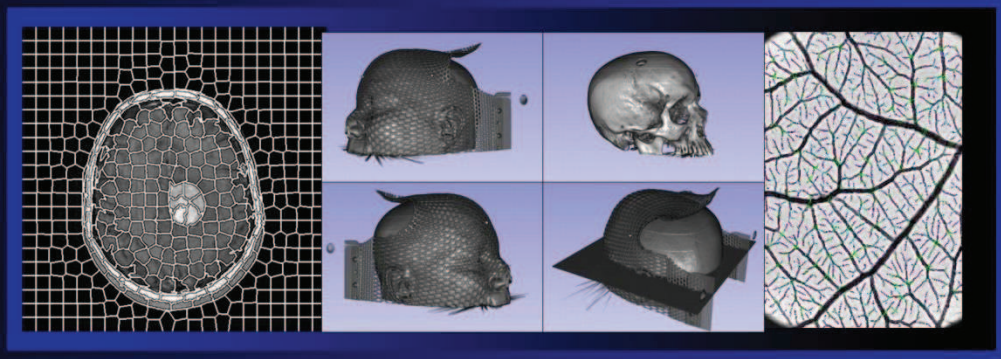

Proceedings of the 19th Conference on Medical Image Understanding and Analysis.
15-17 July 2015
Lincoln, United Kingdom

Automatic Tracking of Retinal Vessel Segments using Radius-Lifted Minimal Path Method

Da Chen
chenda@ceremade.dauphine.fr
Laurent D. Cohen
cohen@ceremade.dauphine.fr

CEREMADE
Université Paris Dauphine
UMR7534, 75016 Paris, France

Abstract

In this paper, we propose an automatic radius-lifted minimal path method to track the retinal vessels fast and accurately. Our method is related to the minimal path technique which is particularly efficient to extract a tubular shape, like a blood vessel. The proposed method consists of a set of pairs of points: each pair of points provides the initial source point and target point. For each pair of such points, we calculate a special anisotropic Riemannian metric with an additional Radius dimension to constrain the fast marching propagation so that our method can get an exact path without any *overlapping extraction*.

1 Introduction

Automatic tracking and analysis of vascular structures is a crucial task in retinal disease diagnostics such as retinopathy of prematurity. In this paper, we deal with the problem of automatically finding a set of radius-lifted minimal paths representing the retinal vessel centreline positions and radii. The minimal path model has been improved deeply since the seminal Cohen-Kimmel model [3], in which tubular structures, or object edges are extracted as the form of minimal paths. This classic model can lead to finding the global minimum with respect to a geodesic energy potential P between two given endpoints. Once this potential is properly defined, Fast Marching (FM) methods [8, 9] are the favored methods to estimate geodesic distances, from which minimal paths can be extracted. However, with Cohen-Kimmel model it is difficult to extract the centreline of the tubular structure and the local width information simultaneously. Li and Yezzi [7] proposed a radius-lifted minimal path technique, defining the potential domain $\hat{\Omega} \subset \mathbb{R}^{n+1}$, connected open and bounded, as the product of spatial space $\Omega \subset \mathbb{R}^n$ with a parameter space $[R_{min}, R_{max}]$ representing vessel radius collection. Thus, each point in the path by [7] contains spatial position and the vessel thickness at this spatial point. Unfortunately, Li-Yezzi model does not take advantage of vessel orientation information which plays an important role in vessel detection. Benmansour and Cohen [1] used an anisotropic Riemannian metric to enhance the Li-Yezzi model. Both Benmansour-Cohen and Li-Yezzi models require the user to give two or more endpoints as the prior knowledge to track the minimal paths. However, for retinal vessel network ex-

traction, it requires considerable user-given endpoints to perform the Benmansour-Cohen model.

The main purpose of this work is to introduce an automatic retinal vessel extraction method, relying on the Benmansour-Cohen model [1] and the vessel skeleton map. A vessel skeleton map is computed by sequential thinning filters [5] to the output of retinal vessel classification methods to obtain the two endpoints for each retinal vessel segment.

2 Background

In this paper, we only consider the 2D vessel extraction so that one point $\mathbf{x} = (x, r) \in \hat{\Omega}$, where $x \in \Omega$ ($\Omega \subset \mathbb{R}^2$) denotes the point position in spatial dimensions and $r \in [R_{min}, R_{max}]$ denotes the position in radius dimension.

Minimal Path and Anisotropic FM with Lattice Basis Reduction: Let $\Im$ denote the collection of Lipschitz paths $\gamma : [0,\ L] \to \hat{\Omega}$. Let s be arc-length parameter, the weighted length through a geodesic energy potential P can be formulated as follows:

$$l_P(\gamma(s)) := \int_0^L \sqrt{\gamma'(s)^T \mathbf{M}(\gamma(s))\gamma'(s)}\, ds, \tag{1}$$

where γ' denotes the tangent vector of path γ. $\mathbf{M}$ is a 3×3 symmetric positive definite tensor defining the anisotropic Riemannian metric [1] in the domain $\hat{\Omega}$. The geodesic distance $\mathscr{U}_{\mathbf{s}}(\mathbf{x})$, is the minimal energy of any path joining $\mathbf{x} \in \hat{\Omega}$ to a given initial point $\mathbf{s}$:

$$\mathscr{U}_{\mathbf{s}}(\mathbf{x}) := \min\{l_P(\gamma) | \gamma \in \Im,\ \gamma(L) = \mathbf{x},\ \gamma(0) = \mathbf{s}\}. \tag{2}$$

The path $C_{\mathbf{s},\mathbf{x}}$ is a *minimal path* if $l_P(C_{\mathbf{s},\mathbf{x}}) = \min_{\gamma}\{l_P(\gamma),\ \gamma \in \Im\}$.

Numerical methods for the geodesic distance map $\mathscr{U}_{\mathbf{s}}(\mathbf{x})$ introduce a discretization grid Z of $\hat{\Omega}$, and for each $\mathbf{x} \in Z$ a small mesh $S(\mathbf{x})$ of a neighborhood of $\mathbf{x}$ with vertices in Z. An approximation of $\mathscr{U}_{\mathbf{s}}$ is given by the solution of the following fixed point problem [8]: find $\mathscr{U}_{\mathbf{s}} : Z \to \mathbb{R}$ such that (i) $\mathscr{U}_{\mathbf{s}}(\mathbf{s}) = 0$ for the initial point $\mathbf{s}$, and (ii) for all $\mathbf{x} \in Z \setminus \mathbf{s}$

$$\mathscr{U}_{\mathbf{s}}(\mathbf{x}) = \min_{\mathbf{y} \in \partial S(\mathbf{x})} \mathscr{P}(\mathbf{x}, \mathbf{y} - \mathbf{x}) + I_{S(\mathbf{x})}\mathscr{U}_{\mathbf{s}}(\mathbf{y}), \tag{3}$$

where $I_{S(\mathbf{x})}$ denotes piecewise linear interpolation on a mesh $S(\mathbf{x})$ [8, 11]. We use the oriented flux filter [6] to detect the retinal vessel orientation. The oriented flux of an image $I : \Omega \to \mathbb{R}^2$, of dimension $d = 2$, is defined by the amount of the image gradient projected along the orientation $\mathbf{p}$ flowing out from a 2D circle at point x with radius r:

$$f(x; r, \mathbf{p}) = \int_{\partial \mathscr{C}_r} (\nabla(G_\sigma * I)(x + r\mathbf{p}) \cdot \mathbf{p})(\mathbf{p} \cdot \mathbf{n}) ds = \mathbf{p}^T \cdot \mathbf{Q}(x, r) \cdot \mathbf{p}, \tag{4}$$

where G_σ is a Gaussian and $\mathbf{n}$ is the outward unit normal vector along $\partial \mathscr{C}_r$. ds is the infinitesimal length of $\partial \mathscr{C}_r$. $\mathbf{Q}(x, r)$ can be considered as the response of oriented flux in (4).

Limitations of Benmansour-Cohen model: Benmansour-Cohen model [1] can accurately extract the vessel boundaries and centrelines at the same time, and also very fast. Unfortunately, despite its numerous advantages, this model exhibits two disadvantages when applied to retinal vessels extraction: (i) it requires user provided endpoints for each tubular structure, which means expensive user intervention; (ii) it may suffer *overlapping extraction* problem (see Fig. 1(c) and (d)).

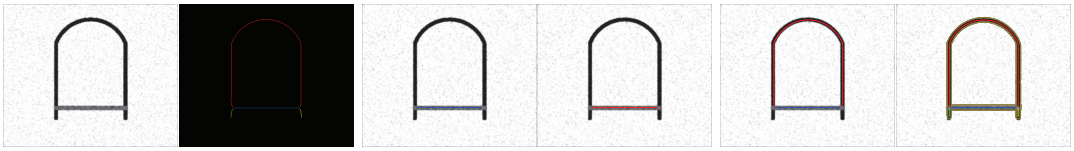

(a) (b) (c) (d) (e) (f)

Figure 1: *overlapping extraction*. (a) Original image. (b) Skeleton map: different segments labeled by different colours. (c)(d) are the results by [1]. (e)(f) are the results by our method.

3 The Proposed Method

3.1 Pre-Processing

In this paper, we use a vessel detector to get the binary segmented map combining with a threshold. Then we thin the binary segmented image by a sequential morphological filters [5] and remove all the branch points. Thus the entire skeleton is broken up into a set of segments. The branch points are defined as any skeleton point having at least three neighbours in its 8-neighborhood. Any endpoint is discovered if it has only one neighbour and segment point has two neighbours. In Fig. 1(b), we show the skeleton map and the labeled segments in different colours. In our work, we firstly scan the entire skeleton map to find all the vessel segments with two endpoints. Delete the segments whose length in pixels are smaller than a given threshold T_{len}. Those segments will be stored in the set $\mathbf{T}$.

3.2 Constrained Riemannian Metric and Anisotropic Fast Marching

We have all the segments and the corresponding endpoints stored in $\mathbf{T}$, in which each segment consists of two endpoints. For each segment $\hbar \in \mathbf{T}$ with two endpoints p_s and p_e, the centreline can be extracted by Benmansour-Cohen model [1] by taking one of the two endpoints as initial point and track the path from another one. However, sometimes *overlapping extraction* will occur and some segments will be missed. In Fig. 1(c), the extracted path follows the segment labeled as blue in Fig 1(b). But the path in Fig. 1(d) is an overlapping extraction path. To solve this problem, we use the following function with respect to $\hbar \in \mathbf{T}$:

$$D_\hbar(x,r) = \begin{cases} 1, & \text{if } d_\hbar(x,r) \leq \ell; \\ +\infty, & \text{else}, \end{cases} \tag{5}$$

where ℓ is a given positive constant. And $d_\hbar(x,r)$ is a distance function:

$$d_\hbar(x,r) = \min_{x_\hbar \in \hbar} \|x - x_\hbar\|_2. \tag{6}$$

representing the minimal Euclidean distance from spatial point $x \in \Omega$ to the segment $\hbar$. $D_\hbar$ in (5) gives an offset region computed by $d_\hbar$ and ℓ. Now we can construct the constrained Riemannian Metric for segment $\hbar \in \mathbf{T}$ as follows:

$$\mathbf{M}_\hbar(\mathbf{x}) = \begin{pmatrix} D_\hbar(\mathbf{x}) & \mathbf{0} \\ \mathbf{0} & D_\hbar(\mathbf{x}) \end{pmatrix} \begin{pmatrix} \tilde{\mathbf{M}}(\mathbf{x}) & \mathbf{0} \\ \mathbf{0} & P_r(\mathbf{x}) \end{pmatrix} = \begin{pmatrix} \left(D_\hbar \cdot \tilde{\mathbf{M}}\right)(\mathbf{x}) & \mathbf{0} \\ \mathbf{0} & \left(D_\hbar \cdot P_r\right)(\mathbf{x}) \end{pmatrix}. \tag{7}$$

The anisotropic entry [1] $\tilde{\mathbf{M}}(x,r)$, which is a 2×2 symmetric definite positive matrix, at point $\mathbf{x} = (x,r)$ can be constructed by $\mathbf{v}_1$, $\mathbf{v}_2$, λ_1 and λ_2, which are the the eigenvectors and

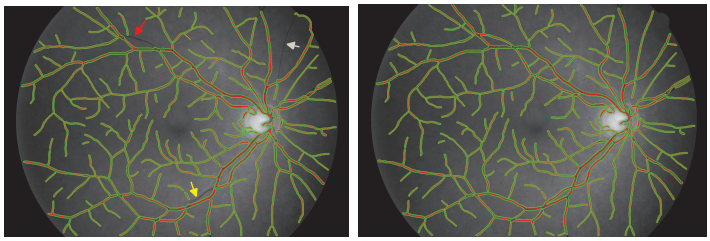

(a) (b)

Figure 2: Segmentation Results.(a) result from [1]. (b) results from the proposed method.

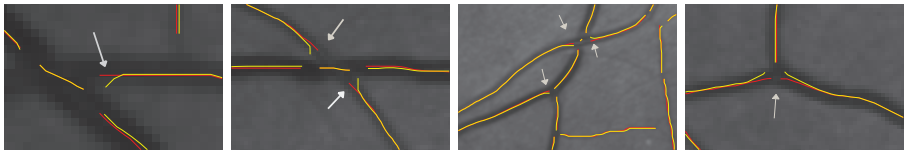

Figure 3: Examples after Endpoints Correcting(see text).

eigenvalues of the response of the oriented flux shown in (4) as:

$$\tilde{\mathbf{M}}(\mathbf{x}) = e^{\alpha\cdot\lambda_2(\mathbf{x})}\mathbf{v}_1(\mathbf{x})\mathbf{v}_1(\mathbf{x})^T + e^{\alpha\cdot\lambda_1(\mathbf{x})}\mathbf{v}_2(\mathbf{x})\mathbf{v}_2(\mathbf{x})^T. \tag{8}$$

The isotropic entry $P_r(\mathbf{x})$ can be computed as [1]:

$$P_r(\mathbf{x}) = \beta \exp\left(\alpha \frac{\lambda_1(\mathbf{x}) + \lambda_2(\mathbf{x})}{2}\right), \tag{9}$$

where α controls the spatial anisotropic ratio while β controls the radius speed. Using the radius-lifted Riemannian metric shown in (7), we can perform the anisotropic FM [8] to transform the Riemannian metric map to distance map. Thus we can find the global minimum with the given constrained metric and initial source point. Note that we give only one physical space endpoint $p_e \in \Omega$. Once the anisotropic FM front meets one point $\mathbf{p} = (p_0, r)$ which follows $p_0 = p_e$, we consider $\mathbf{p}$ to be the endpoint.The radius-lifted path γ, consisting of centreline positions and radii, can be extracted by solving an ODE:

$$\gamma'(s) \propto -\mathbf{M}_{\hbar}^{-1}(\gamma(s)) \cdot \nabla \mathscr{U}(\gamma(s)) \tag{10}$$

Fig. 1(e) and (f) demonstrate the result of our method. In Fig. 2, we show the results of a retinal image from Benmansour-Cohen model and the proposed method respectively. It can be seen that our method can overcome the *overlapping extraction* problem.

3.3 Endpoints Correcting

Sometimes the endpoints of the segment $\hbar$ are not located at the exact centreline of the tubular structure. As an example, see the two endpoints of the segment in Fig. 1(b) labeled as red. We propose an endpoint correcting (EC) method to solve this problem before applying the proposed method described in Section 3.2. The EC method relies on the Euclidean length map Λ of the minimal path. We firstly introduce the Euclidean length calculation method during the FM propagation [2]: an approximation of Λ is the solution of the fixed point

Table 1: Comparison of the proposed model and Benmansour-Cohen model on the test set of DRIVE database.

Methods	Maximum	Minimum	Mean	Standard deviation
Benmansour-Cohen model[1]	0.947	0.9271	0.9372	0.0054
Proposed Method	0.949	0.9305	0.9397	0.0052

problem: find $\Lambda : Z \to \mathbb{R}$ such that (i) for $\mathbf{p}_s \in \hat{\Omega}$, $\Lambda(\mathbf{p}_s) = 0$, and (ii) for all $\mathbf{x} = (x_0, r_0) \in Z \setminus \mathbf{p}_s$, let $\mathbf{y}_\mathbf{x} = (y, r)$ be the point at which the minimum (3) is attained:

$$\Lambda(\mathbf{x}) = \|y - x_0\|_2 + I_{S(\mathbf{x})}\Lambda(\mathbf{y}_\mathbf{x}), \tag{11}$$

Then a single pass solver is possible: whenever the FM updates $\mathscr{U}$, update Λ at the same time, by using the just computed minimizer $\mathbf{y}_\mathbf{x}$ from (3).

The EC method can be described as: for a given segment $\hbar \in \mathbf{T}$ and its two endpoints p_s, p_e we find its middle point $p_m \in \hbar$ and compute the Riemannian metric by (7) as input. Launch the FM from $\mathbf{p}_m = (p_m, 1)$ to compute the maps $\mathscr{U}$ and Λ. Once either endpoint $\tilde{\mathbf{p}}_e = (p_e, r_e)$ is reached, search the desired point inside a set $\mathbf{B} : \{\mathbf{x} \in \hat{\Omega}, \|\mathbf{x} - \tilde{\mathbf{p}}_e\|_2 \leq r_\mathbf{B}\}$ according to the criteria: find a collection of points $\Phi := \{\mathbf{x} \,|\Lambda(\mathbf{x}) \geq [\Lambda(\tilde{\mathbf{p}}_e)] + 1, \mathbf{x} \in \mathbf{B}\}$ where $[n]$ means the largest integer which is smaller than $n \in \mathbb{R}$. Then the desired endpoint can be selected as $\mathbf{p}_e = \arg\min_{\mathbf{x}\in\Phi} \mathscr{U}(\mathbf{x})$. After another endpoint with the same criteria is corrected, stop the algorithm completely. The criteria are based on the fact that among all the points with the same curve length λ, any point which is located at the centreline of the tubular structure has a local minimum arrival time. Fig. 3 shows some details from Fig. 2(b) that the results are improved after endpoint correcting. In Fig. 3, yellow lines indicate the centrelines before endpoint correcting while red lines indicate the centrelines after endpoint correcting.

4 Experiments

In Figs 1 and 2 we have shown the performance of the proposed method. In those two images, the pre-segmented maps are obtained by Hessian-based filter [4]. In the following experiments we will also use this filter to get the pre-segmented maps. For evaluation we apply our method on 20 retinal images got from the test set of the DRIVE dataset [10], acquired through a Canon CR5 non-mydriatic 3CCD camera with a 45 degree field of view (FOV). We show the comparison between Benmansour-Cohen model [1] and our method in Table 1 with evaluation measure Accuracy, which can be computed by the ratio of the summation of the statistical components: the true positive and the true negative to the total number of pixels in the FOV. In this paper, we erode the FOV region by 11 pixels to remove the effect of the boundaries of the FOV to the vessel pre-segmentation. We evaluate our results only inside this eroded FOV region. In Table 2 we show the computational time (CPU) of our algorithm in endpoints correcting and constrained Fast Marching respectively. We also compare the CPU with Benmansour-Cohen model [1] with the same given segment set in the test set of DRIVE. Our method can achieve almost 2 times faster than [1]. In this experiment, we use the parameters as: anisotropic ratio $\mu = 15$, $\beta = 1$, the region offset size ℓ shown in (5) equals 3.

Table 2: CPU (in Seconds) of the proposed model and Benmansour-Cohen model [1] on the test set of DRIVE database.

	Maximum	Minimum	Mean	Standard deviation
Benmansour-Cohen model	22.6	9.16	13.17	3.2
Endpoints Correcting	5.1	4.0	4.39	0.27
Constrained Fast Marching	5.6	4.4	5.06	0.353

5 Conclusions

In this paper, we propose a new tubular structure extraction method based on the constrained anisotropic FM, and introduce an endpoints correcting method using Euclidean curve length. These ingredients allow our method to approximate piecewise minimal paths from complex tubular network, leading better extraction results compared to the Benmansour-Cohen model.

References

[1] F. Benmansour and L. D. Cohen. Tubular Structure Segmentation Based on Minimal Path Method and Anisotropic Enhancement. *IJCV*, 92(2):192–210, 2011.

[2] D. Chen, L. Cohen, and Jean-Marie Mirebeau. Vessel Extraction using Anisotropic Minimal Paths and Path Score. *In Proc: ICIP*, pages 1570–1574, 2014.

[3] L. D. Cohen and R. Kimmel. Global minimum for active contour models: A minimal path approach. *IJCV*, 24(1):57–78, 1997.

[4] A. F. Frangi, W. J. Niessen, Koen L. Vincken, and Max A. Viergever. Multiscale vessel enhancement filtering. *In MICCAI*, pages 407–433, 1998.

[5] Louisa Lam, Seong-Whan Lee, and Ching Y. Suen. Thinning Methodologies - A Comprehensive Survey. *IEEE Transactions on PAMI*, 14(9):869–885, 1992.

[6] Max W. K. Law and Albert C. S. Chung. Three Dimensional Curvilinear Structure Detection Using Optimally Oriented Flux. *In ECCV*, pages 368–382, 2008.

[7] H. Li and A. Yezzi. Vessels as 4-D curves: Global minimal 4-D paths to extract 3-D tubular surfaces and centrelines. *IEEE Trans. Med. Imaging*, 26(9):1213–1223, 2007.

[8] Jean-Marie Mirebeau. Anisotropic Fast-Marching on cartesian grids using Lattice Basis Reduction. *SIAM J. Numer. Anal.*, 52(4):1573–1599, 2014.

[9] J. A. Sethian. Fast marching methods. *SIAM Review*, 41(2):199–235, 1999.

[10] J. Staal, M. D.Abrámoff, M. Niemeijer, M. A. Viergever, and B. V. Ginneken. Ridge based vessel segmentation in color images of the retina. *IEEE Trans. Med Imaging*, 23 (4):501–509, 2004.

[11] J. N. Tsitsiklis. Efficient algorithms for globally optimal trajectories. *IEEE Transactions on Automatic Control*, 40(9):1528–1538, 1995.